IOP Conf. Series: Materials Science and Engineering **263** (2017) 062014 doi:10.1088/1757-899X/263/6/062014

Soret and Dufour effects on MHD non-Darcian radiating convective flow of micropolar fluid past an inclined surface with non-uniform surface heat source or sink and chemical reaction

P Sreenivasulu[1], T Poornima[2] and P Bala Anki Reddy[2]
[1]Department of Humanities and Sciences, SVCET, Chittoor, Andhra Pradesh, India
[2]Department of Mathematics, School of Advanced Sciences, VIT University, Vellore-632014, India

E-mail: bala.anki@vit.ac.in

Abstract. The present study investigates the effects of Soret and Dufour on MHD non- Darcy convective flow of a viscous incompressible radiating micropolar fluid past an inclined permeable plate with non-uniform heat source or sink and chemical reaction. The flow field with partial differential equations are converted to a system of nonlinear coupled ordinary differential equations by similarity transformations and solved employing shooting method. Swiftness in the momentum of the fluid is observed as the Darcian and fluid parameter ascends. Speed of the fluid in angular rotation ascends as the material parameter or sheet inclination or magnetic parameter increases. Molecular diffusion rate is more as the microparticles undergo chemical reactions. While the thermal distribution rate reduces because of the reactions. Rest of the results are interpreted graphically. A good agreement is observed with the previous publications. The presence of chemical reaction makes the problem industrially applicable taking the case of heterogeneous reactions.

1. Introduction

Eringen initiated the concept of polar fluids, especially micro particles suspended fluids whose continuum theory includes local deformations of the particles as a whole particle not in molecular point of view[1-2]. Theory of micropolar fluid has received a considerable attention as it reduces to traditional Newtonian fluids also. Micropolar fluids are non-Newtonian fluids consisting of dumbbell molecules. Dust/ smoke, thin air film can be effectively modelled using theory of micropolar fluids. A bench mark works have been made on micropolar fluids [3-5] Heat generation effects on micropolar fluid past a permeable channel was explained by Singh and Manoj [6]. Qasim [7] presented the effect of heat transfer in a micro-polar fluid over a stretching sheet with Newtonian heating.

Diffuso-thermo or the Dufour effect or otherwise termed as energy fluxes caused due to the temperature variations created by species gradients. Soret effect is the reciprocal of Dufour and is termed as thermo-diffuso effect corresponds to the thermal gradient force due to mobility of particles in mixtures. Since our fluid is a micro-particle immersed fluid, these two effects are much significant. These modes of effects are expected in all steps of matter especially in the mixtures of aerosol and in the fields of geosciences/hydrology. Increased novel works in the thermophoretic effects can be seen in the analysis of convective processes in both clear fluids and porous media. Srinivasacharya and

Upender [8] explained the properties of micropolar fluids with Soret and Dufour effects. Postelnicu [9] examined the influence of chemical reaction along with the thermos-diffuso and diffuso-thermo effects on a viscous flow past vertical surfaces. Mishra *et al.* [10] explained the phenomenon of chemical reaction in micropolar fluids with MHD effects in addition with Soret effects. Sreenivasulu and Bhaskar Reddy [11] explained the effects of diffuso-thermo and thermos-diffuso on MHD radiative flow with dissipation.

Usually through chemical reactions, all cheaper industrial raw materials are designed to transform high value products. Two types of chemical reaction are utilised in general. First and second order chemical reactions can be analysed. Senapati *et al.* [12] investigated the chemical reaction effects on convective flow past a vertical sheet. Poornima *et al.* [13] studied nalysed the chemical reaction effects MHD mixed radiative boundary layer flow past a circular cylinder. Jaffar *et al*. [14] investigated the heat and mass transfer effects on micropolar fluid with radiation and chemical reaction.

With the above awareness, the aim of the present paper is to investigate the influence of diffuse-thermo and chemical reaction effects on MHD micropolar fluid past a stretching sheet imbedded in non-Darcian medium.

2. Mathematical analysis

Consider a mixed convective two dimensional electrically conducting micropolar fluid with radiation and chemical reaction in a steady state. Along the inclined porous plate, the x-axis is taken. The acceleration of gravity g is in a direction opposite to x-coordinate. Transverse magnetic field of strengthB_0 is applied to the plate. Viscous and Darcy resistance terms are taken into account as the constant permeability porous medium. Boussinesq's approximation for the flow modelling is given by

$$\frac{\partial u}{\partial x}+\frac{\partial v}{\partial y}=0 \tag{1}$$

$$u\frac{\partial u}{\partial x}+v\frac{\partial u}{\partial y}=\left(\nu+\frac{k_1}{\rho}\right)\frac{\partial^2 u}{\partial y^2}+g\beta_f(T-T_\infty)\mathrm{Cos}\,\alpha+ g\beta_c(C-C_\infty)\mathrm{Cos}\,\alpha-\frac{\nu\varphi}{k}u-\frac{C_b\varphi}{\sqrt{k}}u^2-\frac{\sigma B_0^2}{\rho}u+\frac{k_1}{\rho}\frac{\partial\omega}{\partial y} \tag{2}$$

$$\rho j\left(\frac{\partial\omega}{\partial x}+v\frac{\partial\omega}{\partial y}\right)=\gamma\frac{\partial^2\omega}{\partial y^2}-k_1\left(2\omega+\frac{\partial u}{\partial y}\right) \tag{3}$$

$$u\frac{\partial T}{\partial x}+v\frac{\partial T}{\partial y}=\frac{1}{\rho Cp}\frac{\partial}{\partial y}\left(K\frac{\partial T}{\partial y}\right)-\frac{1}{\rho Cp}\frac{\partial q_r}{\partial y}+\frac{\sigma B_0^2}{\rho Cp}u^2+\frac{q'''}{\rho Cp}+\frac{\mu}{\rho Cp}\left(\frac{\partial u}{\partial y}\right)^2+\frac{D_m K_T}{C_s C_p}\frac{\partial^2 C}{\partial y^2} \tag{4}$$

$$u\frac{\partial C}{\partial x}+v\frac{\partial C}{\partial y}=D_m\frac{\partial^2 C}{\partial y^2}+\frac{D_m K_T}{T_m}\frac{\partial^2 T}{\partial y^2}-K_c(C-C_\infty) \tag{5}$$

Respective boundary conditions are:

$$u=u_w=bx,\ V=0,\ \omega=-m_0\frac{\partial u}{\partial y},\ T=T_w=T_\infty+A_0\left(\frac{x}{l}\right)^2,\ C=C_w=C_\infty+A_1\left(\frac{x}{l}\right)^2\ at\ y=0$$
$$u\to 0,\quad \omega\to 0,\quad T\to T_\infty,\quad C\to C_\infty \qquad as\quad y\to\infty \tag{6}$$

where u, v are the momentum components along x and y directions, respectively, T is the temperature of the fluid, T_w, T_∞ - the wall and ambient temperature, C is the concentration of the fluid, C_w, C_∞- the wall and ambient concentration, k- the permeability of the porous medium, q_r - the radiative heat flux.μ, p, ν, ρ,α, β_f and β_c are the dynamic viscosity, pressure, kinematic viscosity, density, thermal diffusivity, thermal and solutal expansion coefficients of the fluid respectively. Furthermore σ, B_0 and Cp are electrical conductivity, magnetic induction and the specific heat at constant pressure, respectively. φ, Dm ,T_m , C_s- the porosity ,effective diffusion coefficient, mean fluid temperature, concentration susceptibility, K_T, Kr- the thermal diffusion ratio, chemical reaction rate, g,j,ω,γ- the gravity, inertial density, angular velocity component, spin-gradient viscosity and k_1 is the vortex viscosity.

Rosseland approximation for the radiative heat flux q_r is $q_r = -\frac{4}{3}\frac{\sigma_s}{k_e}\frac{\partial T^4}{\partial y}$ (7)

as the analysis is limited to optically thick fluids. Using Taylor's series, expanding T^4 about the point T_∞ and excluding the higher order terms the following form can be observed:

$$T^4 \cong 4T_\infty^3 T - 3T_\infty^4 \tag{8}$$

Equation (4), in view of equations (7) and (8) turns to

$$u\frac{\partial T}{\partial x} + v\frac{\partial T}{\partial y} = \frac{1}{\rho Cp}\frac{\partial}{\partial y}\left(\left(\kappa + \frac{16T_\infty^3\sigma_s}{3k_e}\right)\frac{\partial T}{\partial y}\right) + \frac{\sigma B_0^2}{\rho Cp}u^2 + \frac{q'''}{\rho Cp} + \frac{\mu}{\rho Cp}\left(\frac{\partial u}{\partial y}\right)^2 + \frac{D_m K_T}{C_s C_p}\frac{\partial^2 C}{\partial y^2} \tag{9}$$

The non-uniform heat source/sink q''' has been taken as

$$q''' = \frac{Ku_w}{x\nu}\left(Q_0\left(T_w - T_\infty\right)e^{-\eta} + Q_1\left(T - T_\infty\right)\right) \tag{10}$$

Defining the spin gradient viscosity which in terms of viscosity and micro-inertia given as

$$\gamma = \left(\mu + \frac{k_1}{2}\right)j = \mu j\left(1 + \frac{K}{2}\right), \qquad K = \frac{k_1}{\mu} \tag{11}$$

Taking the thermal conductivity κ as linearly with temperature and takes the form $\kappa = \kappa_\infty(1 + \varepsilon\theta(\eta))$, where $\theta(\eta) = (T - T_\infty)/(T_w - T_\infty)$ and $\varepsilon = (\kappa_w - \kappa_\infty)/\kappa_\infty$,

which depends on the nature of the fluid and is a small parameter. In general $\varepsilon > 0$ is for air and liquids such as water, while $\varepsilon < 0$ for fluids such as lubrication oils.

Introducing the following similarity transformations,

$$u = bxf'(\eta), v = -\sqrt{b\nu}\,f(\eta), \eta = \sqrt{\frac{b}{\nu}}y, \omega = bx\sqrt{\frac{b}{\nu}}g(\eta), \phi(\eta) = \frac{C - C_\infty}{C_w - C_\infty}, Kr = \frac{K_c}{b}, M = \frac{\sigma B_0^2}{\rho b},$$

$$T - T_\infty = A_0\left(\frac{x}{l}\right)^2\theta(\eta), T_w - T_\infty = A_0\left(\frac{x}{l}\right)^2, C - C_\infty = A_1\left(\frac{x}{l}\right)^2\phi(\eta), C_w - C_\infty = A_1\left(\frac{x}{l}\right)^2, Da^{-1} = \frac{\varphi\nu}{kb}, \tag{12}$$

$$\alpha = \frac{c_b\varphi}{\sqrt{k}}x, \Pr = \frac{\mu Cp}{k_\infty}, Ec = \frac{b^2l^2}{A_0 Cp}, Du = \frac{D_m K_T}{C_s C_p \nu}\frac{(T_w - T_\infty)}{(C_w - C_\infty)}, R = \frac{16\sigma_s T_\infty^3}{3k_e k_\infty}, Sr = \frac{D_m K_T}{T_m \nu}\frac{(T_w - T_\infty)}{(C_w - C_\infty)}$$

In view of equations (9)-(12), the equations (2), (3), (4) and (9) reduce to the dimensionless form:

$$(1+K)f''' + ff'' - (1+\beta)f'^2 - (Da^{-1} + M)f' + kg' + Gr\theta\cos\alpha + Gc\phi\cos\alpha = 0 \tag{13}$$

$$\left(1 + \frac{K}{2}\right)g'' - K(2g + f'') + fg' - f'g = 0 \tag{14}$$

$$(1 + R + \varepsilon\theta)\theta'' + \Pr(f\theta' - 2f'\theta) + \varepsilon\theta'^2 + \Pr MEcf'^2 + \Pr Ecf''^2 + (1 + \varepsilon\theta)(Q_0 f' + Q_1\theta) + \Pr Du\phi'' = 0 \tag{15}$$

$$\phi'' + Sc(f\phi' - 2f'\phi) + ScSr\theta'' - ScK_r\phi = 0 \tag{16}$$

The corresponding boundary conditions are

$$f(0) = 0, \quad f'(0) = 1, \quad g(0) = -m_0 f''(0), \quad \theta(0) = 1, \quad \phi(0) = 1$$
$$f'(\infty) \to 0, \quad g(\infty) \to 0, \quad \theta(\infty) \to 0, \quad \phi(\infty) \to 0 \tag{17}$$

where K is the materiald parameter, Da^{-1} -the inverse Darcy number, M - the magnetic, Gr and Gc are the thermal and solutal Grashof number, Pr -Prandtl number, R, Ec, Du, Sc, Sr, K_r are the radiation parameter, Eckert number, Dufour number, Schmidt number, Soret number and chemical reaction, respectively.

Engineering quantities of our interest are calculated as follows:

Shear stress at wall :

$$\tau_w = \left((\mu + k_1) \frac{\partial u}{\partial y} \right)_{y=0} \quad and \quad C_f = \frac{\tau_w}{\rho u_w^2 / 2} \Rightarrow C_f \, \mathrm{Re}_x^{1/2} = (1+K) f''(0) \tag{18}$$

Couple stress at wall :

$$M_w = \left(\gamma \frac{\partial \omega}{\partial y} \right)_{y=0} \quad and \quad C_m = \frac{M_w}{\mu j u_w} = \left(1 + \frac{K}{2} \right) g'(0) \tag{19}$$

Local Heat transfer rate :

$$Nu_x = \frac{q_w x}{k(T_w - T_\infty)}, \quad where \; q_W = -k \left(\frac{\partial T}{\partial y} \right)_{y=0} \quad and \quad Nu_x \, \mathrm{Re}_x^{-1/2} = -\theta'(0) \tag{20}$$

Local Sherwood number :

$$Sh_x = \frac{j_w x}{D_m (C_w - C_\infty)}, \quad where \; j_W = -D_m \left(\frac{\partial C}{\partial y} \right)_{y=0} \quad and \quad Sh_x \, \mathrm{Re}_x^{-1/2} = -\phi'(0) \tag{21}$$

3. Results and Discussion

The boundary layer partial differential equations for the flow field are reduced to non-linear, coupled ordinary differential equations using similarity variables. Employing shooting method with RK technique, the system of equations is solved. The results are interpreted through graphs 2-14 and tables 1-2 in this section. Comparative study with the available published work have been made. An excellent covenant is found and it is presented in tables1 and 2.

Figures 2-3 depict the profiles of the velocity, micro-rotation versus material parameter (*K*). The momentum of the flow increases due to the microparticles present in the fluid. But it is observed from figure 3, the spinning of the micro particles dominates the flow and collides the boundary as and then, hence the flow descends in this case.

Influence of magnetic field on the momentum and angular rotation portrayed in figures 4-5. The resistive force produced due to the transverse magnetic field retards the motion at all points of the flow field (Figure 4). Figure 5 shows that micro-rotation of the fluid decreases initially and after the trend reverses. The profiles might have been increasing in the absence of microparticle.

Darcy number's influence on the linear motion and angular momentum can be seen in Figures 6-7.The dimensionless linear momentum of the fluid increases with an intensification of Darcy parameter, since the number of pores are more, the intensity of Darcy parameter becomes more as it is directly proportional to it. The micro-rotation of the fluid shows two different behaviours before and after. Initially it decreases and then it rises and approaches to 0 near the free stream.

From Figures8-9, the plate inclined to several increasing angles, the microrotaion and temperature of the fluid increases. It is because of the fact that the buoyancy retards when the sheet inclines. Whereas the fluid heat reduces due to the thermal diffusion factor. Thus, micro-particles effect has a significant impact on the fluid heat (Figure 9).

The influence of heat generation and absorption is plotted in figures 10-11. Heat source parameter induces the heat generation inside the fluid which obviously increases the nearby boundary layer fluid temperature. Because of the continuous induction of heat into fluid rises the temperature as the thermal circulation is more from the plate to fluid (Figure 10).In these figures, the profiles of fluid with variable thermal conductivity asserts more than its absence. From figure 11, the heat is absorbed by the sheet from fluid, thereby reducing the temperature of the fluid. The profiles with varying thermal conductivity presence pronounce less than that of those with its absence.

Figures 12-13 show the variation of the Soret number on concentration and Dufour number on temperature. As *Sr* (Soret) increases, the solutal concentration increases in the boundary layer region $0 < \eta < 5$(Figure 12). Escalation of Dufour number rises up the temperature of the fluid and pronounces

more than that of the profiles with ε = 0. Figure 14shows chemical reaction parameter K_r effect on the solute concentration. Diffusion of concentration slows down because of the particles undergoes chemical reaction. It is seen in the figure concentration decreases as the reaction is more.

The surface skin friction, couple stress, heat transfer rate and mass transfer rate for various physical parameters are shown in table 3. On observing it, wall stress and couple stress, local Nusselt number and molecular diffusion rate decrease as angle of inclination decreases. Also it is evident that the shear stress at the wall, couple stress and Sherwood number increases while those are decreases with an increase in Dufour number *Du*. From table 3, it is clear that the skin friction, couple stress and thermal distribution rate decreases while the rate of molecular dispersion increases with an rise in Schmidt number. Concentration diffusion rate is more as particles undergoes reactions, whereas rate of heat distribution reduces.

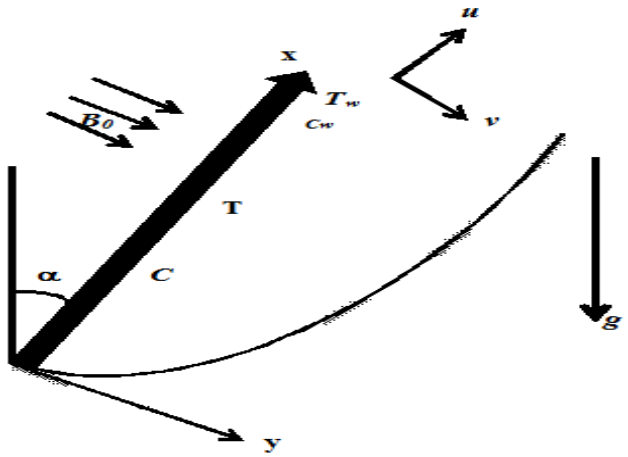

Fig.1 Physical model and coordinate system

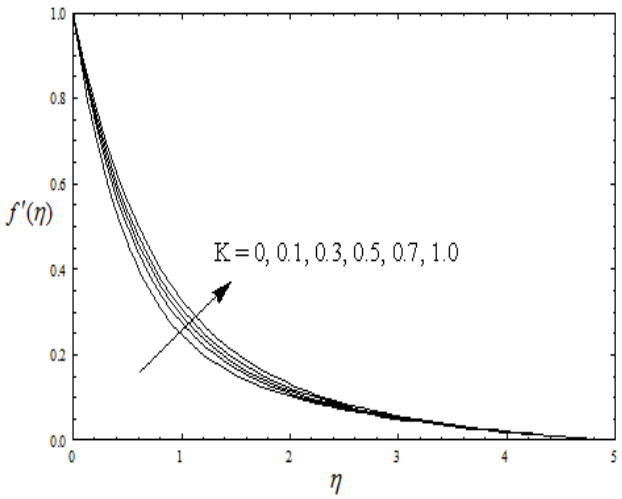

Fig.2 Velocity profiles for different values of *K*

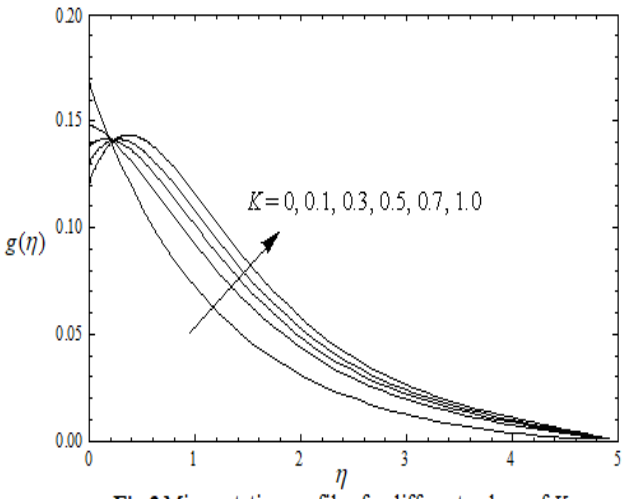

Fig.3 Microrotation profiles for different values of *K*

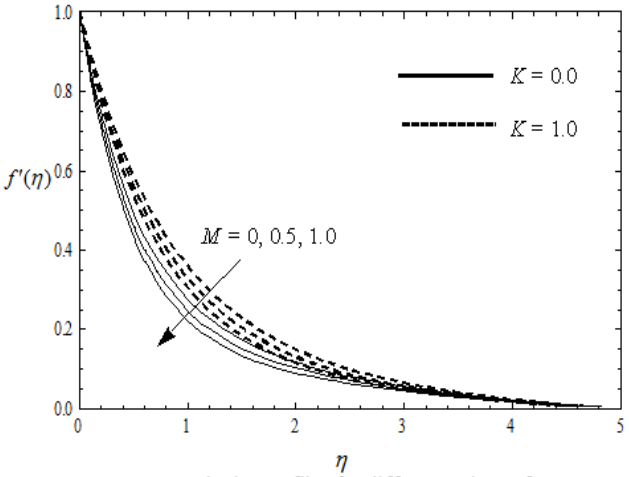

Fig.4 Velocity profiles for different values of M

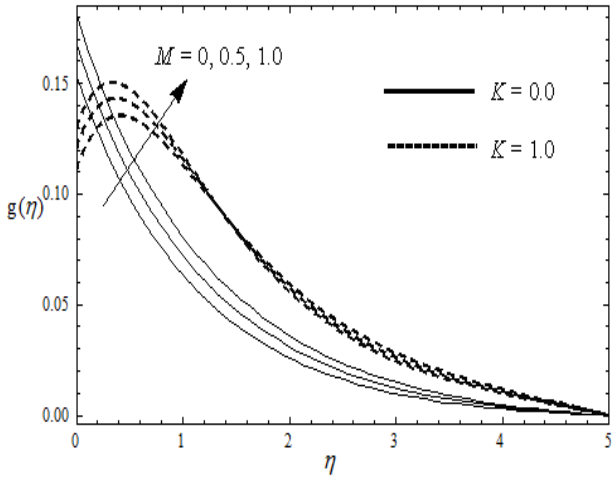

Fig.5 Microrotation profiles for different values of M

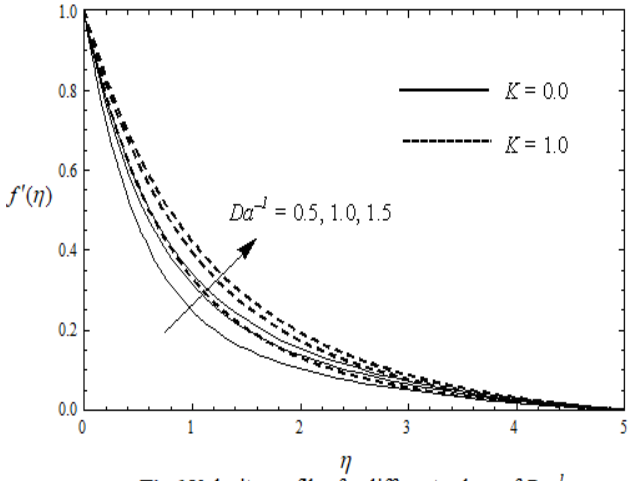

Fig.6 Velocity profiles for different values of Da^{-1}

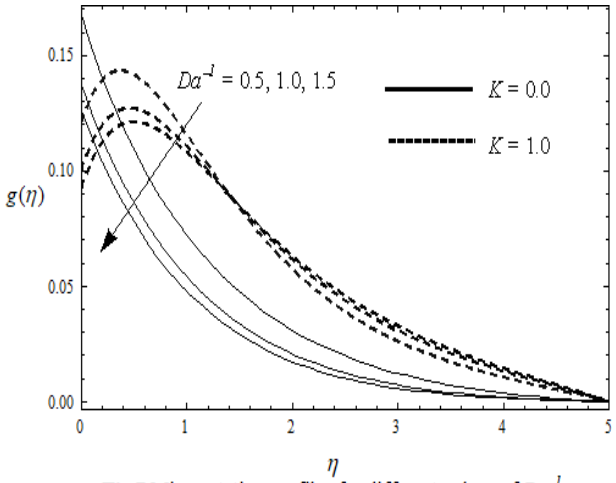

Fig.7 Microrotation profiles for different values of Da^{-1}

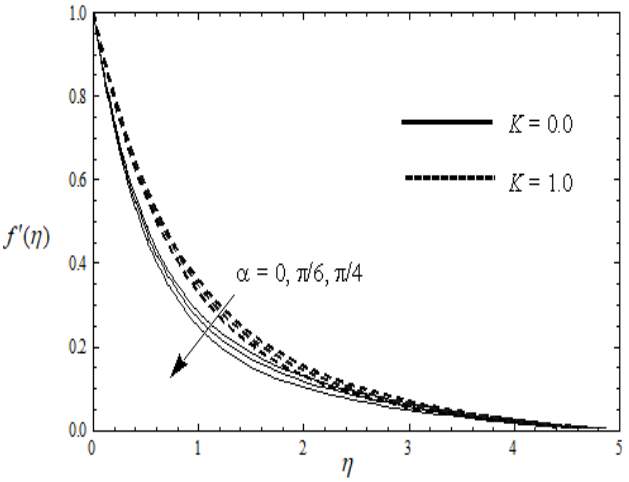

Fig.8 Velocity profiles for different values of α

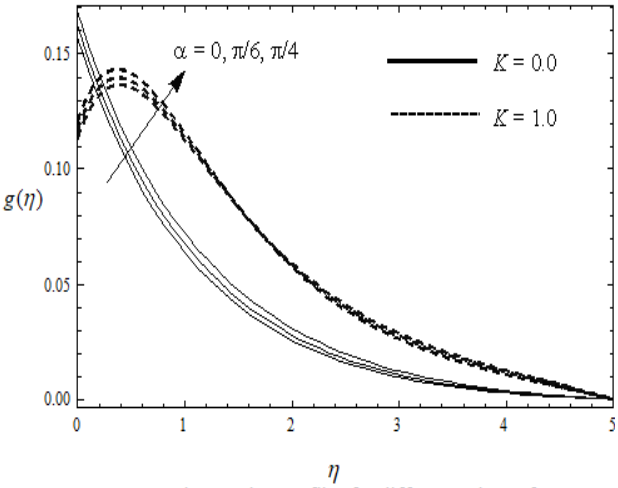

Fig.9 Microrotaion profiles for different values of α

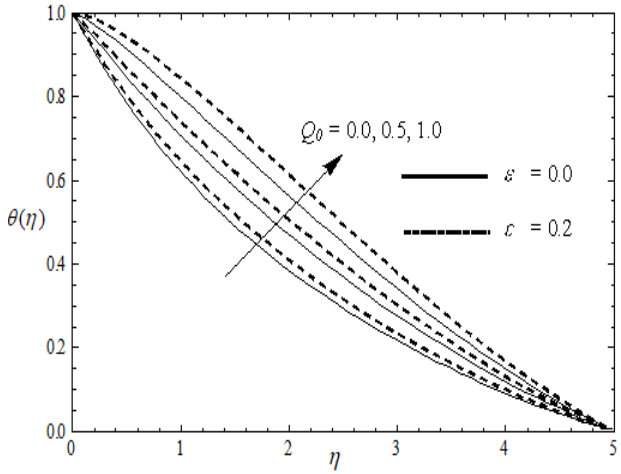

Fig.10 Temperature profiles for different values of Q_0

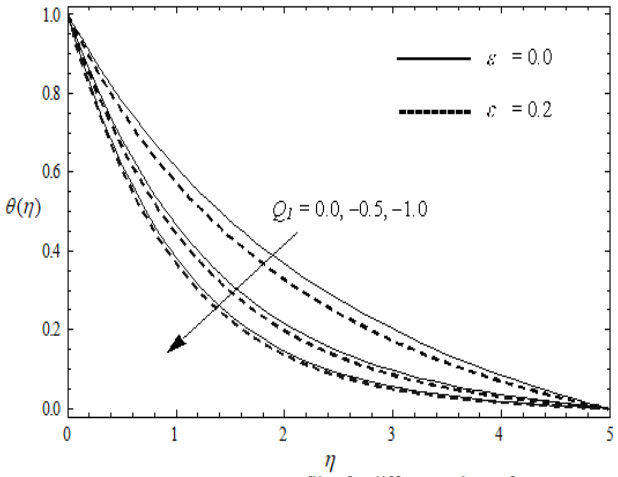

Fig.11 Temperature profiles for different values of Q_1

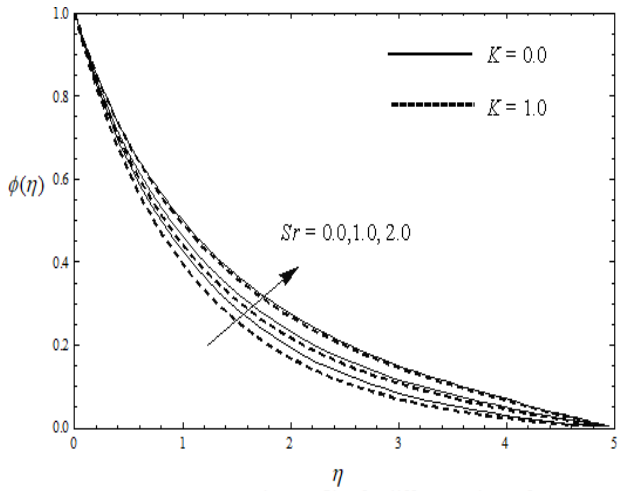

Fig.12 Concentration profiles for different values of Sr

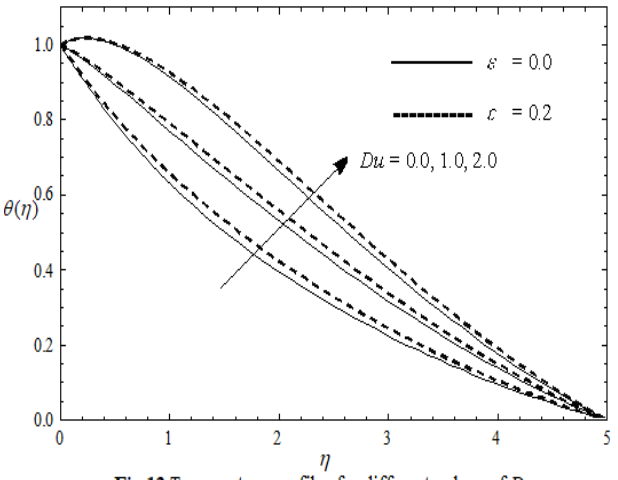

Fig.13 Temperature profiles for different values of Du

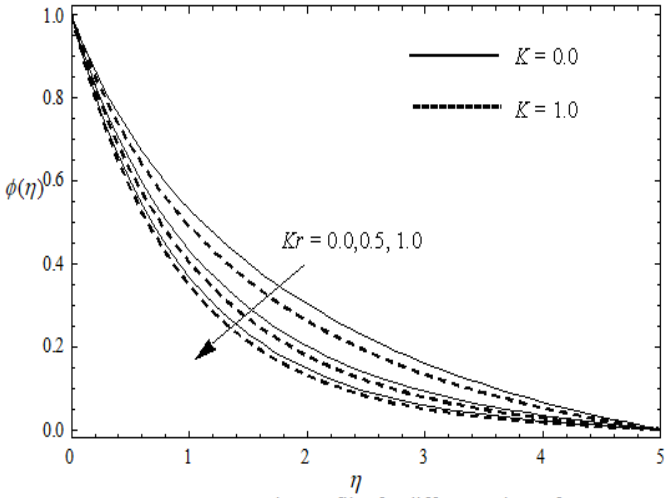

Fig.14 Concentration profiles for different values of Kr

Table 1. Comparison table showing the computations $(1+K)f''(0)$ for different values of *K*.

K	Qasim *et al*. [7]	Maboob *et al.* [3]	R-K method solutions
0.00	-1	-1	– 1.0073
1	– 1.367872	– 1.367996	– 1.3695
2	– 1.621225	– 1.621575	– 1.6228
3	-------	– 1.827382	– 1.8231
4	– 2.004133	– 2.005420	– 2.0040
5	-------	– 2.1648230	– 2.1634

Table 2. Assessment of Nusselt number for different *Pr*.

Pr	Maboob e*t al* [3]	R-K solutions
1	1.33333334	1.3335
3	2.50972157	2.5099
10	4.79687059	4.7978

Table 3. Computations showing data of $f''(0)$, $g'(0)$, $-\theta'(0)$ and $-\phi'(0)$ when $K=\beta=Da^{-1}=Gr=Gc=m_0=Q_0=M=R=\varepsilon=Ec=Sr=0.1, \Pr=1\ Q_0=-1$

α	*Du*	*Sc*	*Kr*	$f''(0)$	$g'(0)$	$-\theta'(0)$	$-\phi'(0)$
0	0.2	0.22	0.5	–1.01716	–0.05639	1.13042	0.44568
π/6	0.2	0.22	0.5	–1.03051	–0.05714	1.12676	0.44468
π/4	0.2	0.22	0.5	–1.04646	–0.05801	1.12231	0.44346
π/4	0.5	0.22	0.5	–1.04498	–0.05791	1.08886	0.44386
π/4	0.8	0.22	0.5	–1.04349	–0.05781	1.05529	0.44426
π/4	1.0	0.22	0.5	–1.04250	–0.05774	1.03283	0.44453
π/4	0.2	0.5	0.5	–1.05548	–0.05790	1.04907	1.00062
π/4	0.2	1	0.5	–1.06061	–0.05791	0.98299	1.48246
π/4	0.2	2	0.5	–1.06514	–0.05797	0.88196	2.18712
π/4	0.2	0.22	0.7	–1.05073	–0.05794	1.09243	0.67466
π/4	0.2	0.22	1.0	–1.05168	–0.05793	1.08591	0.72542
π/4	0.2	0.22	1.2	–1.05225	–0.05792	1.08178	0.75735

4. Conclusions

An analysis is made to study the effect of thermo-diffusion and diffusion-thermo on magnetohydrodynamic micropolar mixed convection non-Darcian flow past an inclined porous surface with chemical reaction and non-uniform surface heat source or sink. Computations are done by shooting method with R-K and the outputs were portrayed through graphs and tables. Significant conclusions are drawn basing on the investigation:

- Presence of micro-polar particles has significant effect rather than its absence.
- Translational and rotational velocity escalates with an escalation in the material parameter.
- Heat transfer through radiation rises the fluid temperature.
- There is a significant rise in the temperature for varying thermal conductivity parameter.
- The species concentration diffusion rate is more because of the reacting particles present inside the fluid.
- Concentration spreads well with intensification of *Sr* and heat also rises up with rising *Du* values.

References

[1] Eringen C 1966 *Journal of Mathematics and Mechanics* **16**1-18
[2] Eringen C 1972 *Journal of Mathematical Analysis and Applications* **38(2)** 480-96
[3] Mabood F, Ibrahim S M, Rashidi M M, Shadloo M S and Giulio Lorenzini2016 *Int. J. Heat and Mass Transfer* **93** 674-682
[4] Siva Reddy Sheri and Shamshuddin MD 2015 *Procedia Engineering***127** 885-92
[5] Sheri Siva Reddy and Shamshuddin MD 2016 *Theoretical and Applied Mechanics* **43(1)** 117–31
[6] Khilap Singh and Manoj Kumar 2016 *Journal of Thermodynamics* **2016**10
[7] Qasim M, Khan I and Shafie S 2013*PLoS ONE* **8(4)** e5939
[8] Srinivasacharya D and Upendar M 2014 *Afrika Matematika* **25(3)**693-705
[9] Adrian Postelnicu 2007*Heat and Mass Transfer* **43**595–602
[10] Mishra S R,Baag S and Mahapatra D K 2016 *Engineering Science and Technology, an Int. J.* **19(4)** 1919-28
[11] Sreenivasulu P and Bhaskar Reddy N 2012 *Advances in Applied Science Research* **3(6)** 3890-901
[12] Senapati N, Dhal R K and Das T K 2012 *American Journal of Computational and Applied Mathematics* **2(3)** 124-35
[13] Poornima T, Sreenivasulu P and Bhaskar Reddy N 2016 *Journal of Applied Fluid Mechanics* **9(6)** 2877-85
[14] Fatin Nur Fatiha Binti Jaafar, Kandasamy Rand Natasha Amira Binti Mohd Zailani 2016 *SCIREA Journal of Mechanical Engineering* **1(1)** 42-57